

# GaInAsP/InP Lateral Current Injection Laser With Uniformly Distributed Quantum-Well Structure

Mitsuaki Futami, Takahiko Shindo, *Student Member, IEEE*, Takayuki Koguchi, Keisuke Shinno, Tomohiro Amemiya, *Member, IEEE*, Nobuhiko Nishiyama, *Senior Member, IEEE*, and Shigehisa Arai, *Fellow, IEEE*

**Abstract**—To enhance the internal quantum efficiency of GaInAsP/InP lateral current injection (LCI) lasers, we adopted a structure consisting of five uniformly distributed quantum-wells (QWs). A differential quantum efficiency of 59% and an internal quantum efficiency of 70% were obtained for a cavity length of 750  $\mu\text{m}$ , the latter value is almost twice that of an LCI-Fabry-Pérot laser with a conventional QW structure.

**Index Terms**—GaInAsP/InP, lateral current injection, quantum-well laser, semiconductor laser.

## I. INTRODUCTION

VERY large-scale integration (VLSI) with sophisticated logic devices is now facing difficulties with signal delay and power consumption in global wiring because the constant chip size prevents the lines from scaling in length. As a promising approach to this problem, photonic integrated circuits (PICs) in LSI have been receiving considerable attention owing to their high-speed, low-loss performance [1], [2]. A critical issue for realization of PICs in LSI is the availability of an ultralow power consumption light source. If we are to integrate optical interconnection into LSI circuits, the maximum power consumption of the light source for on-chip use must be less than 100 fJ/bit [3]. Micro-cavity lasers such as vertical-cavity surface emitting lasers [4]–[7] and microdisk lasers [8], [9] have been reported as very low power consumption light sources. Photonic crystal lasers

are thought to be an especially promising approach, and an ultralow threshold operation under current injection [10] as well as a very high-speed operation under optical pumping [11] has been reported recently.

We have proposed a GaInAsP/InP membrane distributed feedback (DFB) laser consisting of a thin semiconductor core layer sandwiched by polymer claddings such as air, benzocyclobutene, or SiO<sub>2</sub>. The membrane structure produces a large refractive-index difference between the core layer and the cladding layers and supports strong optical confinement to the active region, leading to ultralow power consumption. In our previous report, low threshold (irradiated power: 0.34 mW) and stable single-mode operation under room temperature continuous wave (RT-CW) optical pumping was demonstrated [12], and the device's temperature oscillated up to 85 °C under CW conditions [13]. These experimental results suggested that this membrane structure has great potential as a light source in LSI circuits. To achieve an electrical-injection-type membrane laser, a lateral current injection (LCI) structure was introduced [14], in which the current flows via p-n junctions on either side of the core layer. RT-CW operation of LCI Fabry-Pérot (FP) lasers and DFB lasers on a semi-insulating substrate have been demonstrated [15]–[17]. However, they exhibited a relatively low internal quantum efficiency ( $\eta_i$ ) of around 40%, which was attributed to a large amount of carrier leakage in the optical confinement layers (OCLs). In this letter, we propose and demonstrate a uniformly distributed five-quantum-well structure for LCI-FP lasers in an attempt to address this problem.

## II. DEVICE STRUCTURE

Figure 1(a) schematically illustrates the structure of an LCI-FP laser with five uniformly distributed QWs. The cross-sectional structure of its core layer, which has a total thickness of 400 nm, is shown in Fig. 1(b); that of a conventional core layer having the same total thickness is shown as a reference. The core layer consists of five 1% compressively strained Ga<sub>0.22</sub>In<sub>0.78</sub>As<sub>0.81</sub>P<sub>0.19</sub> QWs, 0.15% tensile-strained Ga<sub>0.26</sub>In<sub>0.74</sub>As<sub>0.49</sub>P<sub>0.51</sub> barriers, and OCLs. The notable feature of this structure is that five QWs are located along the core layer at regular intervals of 45 nm, and OCLs fill the gaps between them.

Manuscript received December 22, 2012; revised February 13, 2012; accepted February 27, 2012. Date of publication April 5, 2012; date of current version April 20, 2012. This work was supported in part by the Ministry of Education, Culture, Sports, Science and Technology (MEXT), Japan, in part by the Japan Society for Promotion of Science (JSPS) under Grants-in-Aid for Scientific Research 19002009, 21226010, 22360138, 21860031, and 10J08973, and in part by the JSPS and the Council for Science and Technology Policy (CSTP) under the FIRST Program. The work of T. Shindo was supported by the JSPS under a Research Fellowship for Young Scientists.

M. Futami, T. Shindo, T. Koguchi, K. Shinno, T. Amemiya, and N. Nishiyama are with the Department of Electrical and Electronic Engineering, Tokyo Institute of Technology, Tokyo 152-8552, Japan (e-mail: futami.m.aa@m.titech.ac.jp; shindou.t.aa@m.titech.ac.jp; koguchi.t.aa@m.titech.ac.jp; shinno.k.aa@m.titech.ac.jp; amemiya.t.ab@m.titech.ac.jp; n-nishi@pe.titech.ac.jp).

S. Arai is with the Department of Electrical and Electronic Engineering, Tokyo Institute of Technology, Tokyo 152-8552, Japan, and also with the Quantum Nanoelectronics Research Center, Tokyo Institute of Technology, Tokyo 152-8552, Japan (e-mail: arai@pe.titech.ac.jp).

Color versions of one or more of the figures in this letter are available online at <http://ieeexplore.ieee.org>.

Digital Object Identifier 10.1109/LPT.2012.2190053

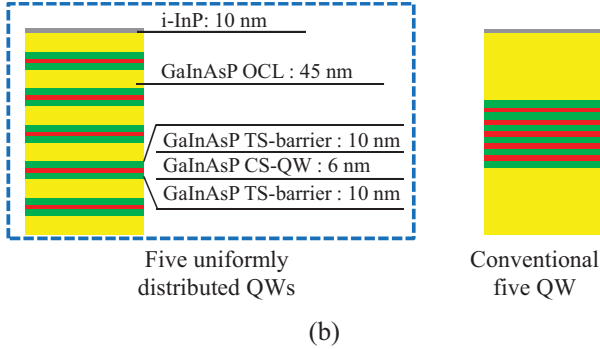
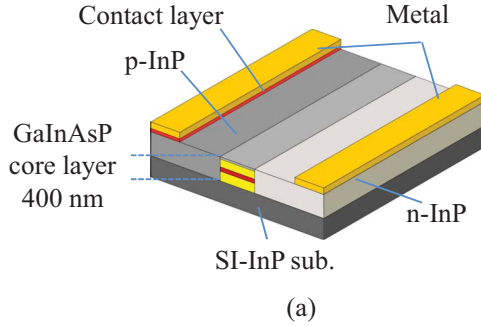


Fig. 1. (a) Schematic device structure and (b) cross-sectional structure of five uniformly distributed QWs (conventional core layer shown as reference).

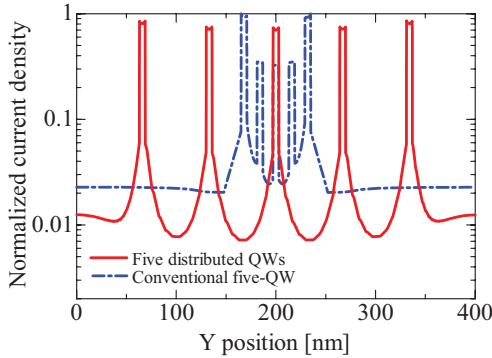


Fig. 2. Current density profiles of the five uniformly distributed QWs and the conventional five-QW structure.

Since the poor internal quantum efficiency of the conventional LCI structure was considered to be due to non-uniform carrier profile in each QW or surface recombination at the top of the OCL, we tried to increase carrier capture into QWs by inserting OCLs between QWs. To confirm this, we calculated the current distribution over the core layers by using a commercial semiconductor device simulator, APSYS, from Crosslight Software Inc. The results are shown in Fig. 2, where the Y position corresponds to the stacking direction of each core layer shown in Fig. 1(b). The simulation results confirmed that the leakage current in the OCLs was smaller in the LCI structure with five uniformly distributed QWs.

The device was fabricated as follows. An initial wafer with undoped GaInAsP containing five uniformly distributed QWs was prepared by organometallic vapor-phase epitaxy (OMVPE) on an Fe-doped semi-insulating (SI) InP substrate.

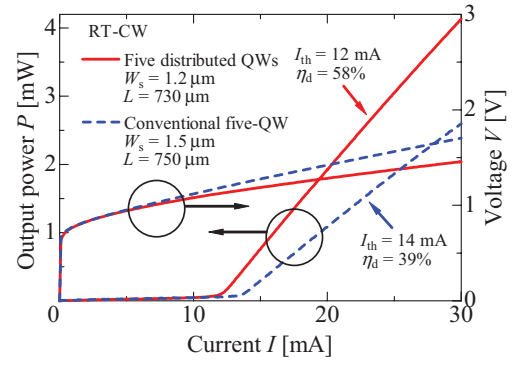


Fig. 3.  $I$ - $L$  and  $I$ - $V$  characteristics of fabricated LCI laser.

The LCI structure was fabricated by  $\text{CH}_4/\text{H}_2$  reactive-ion etching (RIE) and two-step OMVPE selective area growth. First, a mesa stripe  $7 \mu\text{m}$  wide and  $400 \text{ nm}$  high was formed by RIE etching with a  $\text{SiO}_2$  mask, and n-InP ( $N_d = 4 \times 10^{18} / \text{cm}^3$ ) was selectively regrown on both sides of the mesa as a cladding layer. Next, one side of the cladding layer was etched, and p-InP ( $N_a = 4 \times 10^{18} / \text{cm}^3$ ) and the p-GaInAs contact layer ( $N_a = 8 \times 10^{18} / \text{cm}^3$ ) were regrown in the same way. Finally, electrodes were deposited on both the p-contact and n-InP sections.

### III. EXPERIMENTAL RESULTS

Figure 3 shows the light output properties and voltage-current ( $V$ - $I$ ) curves of an LCI laser with five uniformly distributed QWs and a conventional five-QW LCI laser having similar cavity lengths ( $L$ ) and stripe widths ( $W_s$ ) with as-cleaved facets. RT-CW operation was achieved with both LCI lasers, and the laser with uniformly distributed QWs had a higher output efficiency than the conventional laser. The threshold current ( $I_{\text{th}}$ ) and differential quantum efficiency ( $\eta_d$ ) of the uniformly distributed QW type were  $12 \text{ mA}$  and  $59\%$  (both facets), and those of the conventional type were  $14 \text{ mA}$  and  $39\%$ , respectively.

A relatively low  $I_{\text{th}}$  of approximately  $10 \text{ mA}$  was obtained for the lasers with uniformly distributed QWs, which is almost the same value as that of conventional lasers with a vertical injection structure. The lowest  $I_{\text{th}}$ ,  $9.1 \text{ mA}$ , was obtained for a device with a  $480\text{-}\mu\text{m}$ -long cavity. Assuming a uniform carrier density profile along the direction of the stripe, the estimated threshold current density ( $J_{\text{th}}$ ) of the device was  $1.6 \text{ kA/cm}^2$  for a cavity length of  $480 \mu\text{m}$  and  $0.95 \text{ kA/cm}^2$  for a length of  $1050 \mu\text{m}$ . The lasing wavelengths of LCI lasers with uniformly distributed QWs and conventional QWs were  $1580 \text{ nm}$  and  $1530 \text{ nm}$ , respectively.

The  $V$ - $I$  curve of the laser having uniformly distributed QWs (solid line) indicates that the voltage and the differential series resistance near the threshold current were  $1.1 \text{ V}$  and  $21 \Omega$ , respectively; these are almost the same values as those of LCI lasers with conventional QWs (dashed line). The large series resistance is attributed to high contact resistance and high sheet resistance at the p-InP side; it necessitates some modifications of the device design, such as an increase in the hole concentration in the p-InP region.

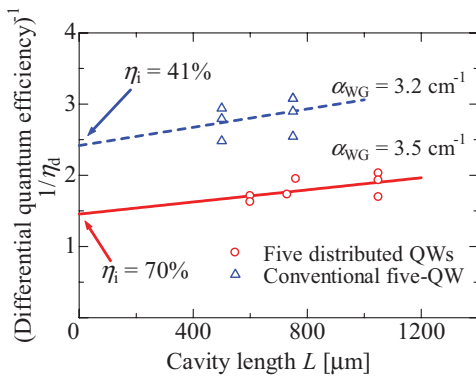


Fig. 4. Differential quantum efficiency as a function of the cavity length.

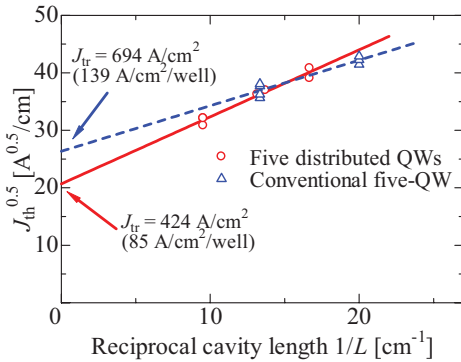


Fig. 5. Square root of threshold current density as a function of the reciprocal cavity length for the LCI lasers.

Figure 4 shows a plot of the reciprocal of the measured  $\eta_d$  versus the cavity length  $L$  and its linear approximation. The solid and dashed lines in this graph represent LCI lasers with uniformly distributed QWs and with a conventional QW structure, respectively. These results revealed a waveguide loss ( $\alpha_{WG}$ ) of  $3.5 \text{ cm}^{-1}$  and an  $\eta_i$  value of 70% for the former, whereas the values for the conventional QW lasers were  $3.2 \text{ cm}^{-1}$  and 41%, respectively. Therefore, the introduction of the uniformly distributed-QW structure significantly improved the internal quantum efficiency of LCI lasers.

Next, the transparent current density ( $J_{tr}$ ) was evaluated using the relationship between the inverse of  $L$  and the square root of  $J_{th}$ , as shown in Fig. 5 [18]. From this result, we obtained a  $J_{tr}$  per well of  $85 \text{ A/cm}^2$  for the uniformly distributed QW structure, which is comparable to that of a vertical current injection type semiconductor laser fabricated in our laboratory [19], whereas that of the conventional QW structure was  $139 \text{ A/cm}^2$ . The improved  $J_{tr}$  value in the uniformly distributed QW structure indicates its superior  $\eta_i$ . This is due to a reduction in leakage carriers, which did not recombine in the QWs. If this uniformly distributed QW structure is applied to injection-type membrane lasers [20], lower threshold operation can be expected.

#### IV. CONCLUSION

An LCI semiconductor laser with five uniformly distributed QWs was successfully demonstrated on an SI-InP substrate. An internal quantum efficiency of 70% was obtained. This value is comparable to that of vertical current injection type semiconductor lasers.

#### ACKNOWLEDGMENT

The authors would like to thank M. Asada, F. Koyama, and T. Mizumoto and Associate Professors Y. Miyamoto and M. Watanabe of the Tokyo Institute of Technology, Tokyo, Japan.

#### REFERENCES

- [1] G. Chen, *et al.*, "Predictions of CMOS compatible on-chip optical interconnect," *Integr. VLSI J.*, vol. 40, no. 4, pp. 434–446, Jul. 2007.
- [2] G. Roelkens, *et al.*, "III-V/silicon photonics for on-chip and intra-chip optical interconnects," *Laser Photon. Rev.*, vol. 4, no. 6, pp. 751–779, Nov. 2010.
- [3] D. Miller, "Device requirements of optical interconnects to silicon chips," *Proc. IEEE*, vol. 97, no. 7, pp. 1166–1185, Jul. 2009.
- [4] K. Iga, "Surface-emitting laser-Its birth and generation of new optoelectronics field," *IEEE J. Sel. Topics Quantum Electron.*, vol. 6, no. 6, pp. 1201–1215, Nov./Dec. 2000.
- [5] N. Nishiyama, *et al.*, "Long-wavelength vertical-cavity surface-emitting lasers on InP with lattice matched AlGaInAs-InP DBR grown by MOCVD," *IEEE J. Sel. Topics Quantum Electron.*, vol. 11, no. 5, pp. 990–998, Sept./Oct. 2000.
- [6] P. Moser, *et al.*, "81 fJ/bit energy-to-data ratio of 850 nm vertical-cavity surface-emitting lasers for optical interconnects," *Appl. Phys. Lett.*, vol. 98, pp. 231106-1–231106-3, Jun. 2011.
- [7] M. C. Y. Huang, Y. Zhou, and C. J. Chang-Hasnain, "A surface-emitting laser incorporating a high-index-contrast subwavelength grating," *Nature Photon.*, vol. 1, no. 2, pp. 119–123, Feb. 2007.
- [8] M. Fujita, R. Ushigome, and T. Baba, "Continuous wave lasing in GaInAsP microdisk injection laser with threshold current of  $40 \mu\text{A}$ ," *Electron. Lett.*, vol. 36, no. 9, pp. 790–791, Apr. 2000.
- [9] D. Van Thourhout, *et al.*, "Nanophotonic devices for optical interconnect," *IEEE J. Sel. Topics Quantum Electron.*, vol. 16, no. 5, pp. 1363–1375, Sep./Oct. 2010.
- [10] B. Ellis, *et al.*, "Ultralow threshold, electrically pumped quantum dot photonic crystal nanocavity laser," *Nat. Photon.*, vol. 5, pp. 297–300, May 2011.
- [11] C.-H. Chen, *et al.*, "Optically injection-locked photonic crystal laser with  $>67 \text{ GHz}$  modulation bandwidth," *Electron. Lett.*, vol. 47, no. 22, pp. 1240–1241, Oct. 2011.
- [12] S. Sakamoto, *et al.*, "Strongly index-coupled membrane BH-DFB lasers with surface corrugation grating," *IEEE J. Sel. Topics Quantum Electron.*, vol. 13, no. 5, pp. 1135–1141, Sep./Oct. 2007.
- [13] S. Sakamoto, *et al.*, "85 °C continuous-wave operation of GaInAsP/InP-membrane buried heterostructure distributed feedback lasers with polymer cladding layer," *Jpn. J. Appl. Phys.*, vol. 46, no. 47, pp. 1155–1157, Nov. 2007.
- [14] K. Oe, Y. Noguchi, and C. Caneau, "GaInAsP lateral current injection lasers on semi-insulating substrates," *IEEE Photon. Technol. Lett.*, vol. 6, no. 4, pp. 479–481, Apr. 1994.
- [15] T. Okumura, *et al.*, "Lateral current injection GaInAsP/InP laser on semi-insulating substrate for membrane-based photonic circuits," *Opt. Express*, vol. 17, no. 15, pp. 12564–12570, Jul. 2009.
- [16] T. Shindo, *et al.*, "GaInAsP/InP lateral-current-injection distributed feedback laser with a-Si surface grating," *Opt. Express*, vol. 19, no. 3, pp. 1884–1891, Jan. 2011.
- [17] T. Shindo, *et al.*, "Lateral-current-injection distributed feedback laser with surface grating structure," *IEEE J. Sel. Topics Quantum Electron.*, vol. 17, no. 5, pp. 1175–1182, Sept./Oct. 2011.
- [18] P. W. A. McIlroy, A. Kurobe, and Y. Uematsu, "Analysis and application of theoretical gain curves to the design of multi-quantum-well layers," *IEEE J. Quantum Electron.*, vol. 21, no. 12, pp. 1958–1963, Dec. 1985.
- [19] T. Shindo, S. Lee, D. Takahashi, N. Tajima, N. Nishiyama, and S. Arai, "Low-threshold and high-efficiency operation of distributed reflector laser with wirelike active regions," *IEEE Photon. Technol. Lett.*, vol. 21, no. 19, pp. 1414–1416, Oct. 1, 2009.
- [20] T. Okumura, T. Koguchi, H. Ito, N. Nishiyama, and S. Arai, "Injection-type GaInAsP/InP membrane buried heterostructure distributed feedback laser with wirelike active regions," *Appl. Phys. Express*, vol. 4, no. 4, pp. 042101-1–042101-3, Mar. 2011.